Dark Modes and Fano Resonances in Plasmonic Clusters Excited by Cylindrical Vector Beams

Jordi Sancho-Parramon[†,‡,*] and Salvador Bosch[†]

[†]Departament de Física Aplicada i Òptica, Universitat de Barcelona, Martí i Franquès 1, 08028, Barcelona, Spain and [‡]Rudjer Boskovic Institute, Bijenicka cesta 54, 10002, Zagreb, Croatia

ABSTRACT Control of the polarization distribution of light allows tailoring the electromagnetic response of plasmonic particles. By rigorously extending the generalized multiparticle Mie theory, we show that focused cylindrical vector beams (CVB) can be used to efficiently excite dark plasmon modes in nanoparticle clusters. In addition to the small radiative damping and large field enhancement associated to dark modes, excitation with CVB can give place to unusual phenomenology like the formation of electromagnetic cold spots and the generation of Fano resonances in highly symmetric clusters. Overall, the results show the potential of CVB to tailor the plasmonic response of nanoparticle clusters in a unique way.

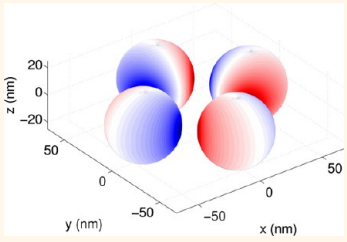

KEYWORDS: surface plasmon resonance · cylindrical vector beams · focused illumination · nanoparticle · plasmon hybridization · subradiance · near-field enhancement · Fano resonance · electromagnetic cold spots

Collective electron oscillations in metal nanoparticles, known as localized surface plasmon resonances, result in strong far-field scattering and near-field enhancement of the excitation radiation.[1,2] Resonances with a net dipole moment are known as bright, as they can easily couple to light, while resonances with a zero dipole moment are named dark.[3] In the quasi-static approximation, the dipole resonance of single particles is bright while the quadrupole resonance is dark. In coupled nanoparticle systems, the hybridization theory[4] introduces in an elegant way bright and dark plasmons as the result of in-phase and out-of-phase coupling of the dipole moments of nanoparticles in dimers. Bright plasmons have been largely studied since they can be simply excited by optical means. However, dark plasmons are receiving a growing interest: owing to its vanishing dipole moment, the reradiation of energy in the far field is significantly smaller than for bright modes, resulting in strong electromagnetic enhancement in the near-field region.[5] Besides, dark resonances present high quality factors due to the small radiative damping.[5] Thus, dark plasmon modes have a large potential for applications such as biological and chemical sensing or wave-guiding in particle chains free of radiative losses.[6,7] Interference between a spectrally narrow dark mode and a broad bright mode can give place to asymmetric line-shapes in the plasmonic spectra of nanostructures,[8] in analogy to the Fano resonances occurring in atomic systems as a result of the coupling of discrete states with a broad continuum.[9] The Fano lineshape has larger sensitivity to the dielectric environment in comparison to other plasmonic resonances,[8] which has led to intense research in design of particle shapes and clusters with strong Fano resonances.[10−14]

Breaking the symmetry of a nanostructure enables rendering dark modes as optically active, yet subradiant, and having large field enhancements and quality factors. This is the case of heterodimers,[15] asymmetric core−shell particles,[13] and rings.[16] In symmetric structures, dark plasmons can be excited by nonoptical means such as electron beams.[3] Generation of dark modes by light requires breaking the excitation symmetry: this can be achieved using inhomogeneous excitation of the nanostructure,[17] evanescent waves,[18] non-normal incidence,[19] retardation effects,[20,21] localized emitters,[5] or spatial phase shaping.[22,23] Actually, control on the phase of light acting on a plasmonic structure enables not only excitation of dark modes but also broad tailoring of its near field response. Thus, control on the location of regions with large light concentration can be achieved by temporal[24] or spatial[25−27] phase modulation of the incident radiation or by using auxiliary plasmonic structures to

* Address correspondence to jsancho@irb.hr.

Received for review July 19, 2012 and accepted August 24, 2012.

Published online August 25, 2012
10.1021/nn303243p

mold the flow of light into a primary system designed for field enhancement.[28,29]

In this work we study the response of plasmonic clusters excited by cylindrical vector beams (CVB), in particular, azimuthally (AP) and radially (RP) polarized beams. The polarization distribution of focused CVB has been shown to have applications in laser machining, optical trapping, or generation of surface plasmon polaritons in metal-dielectric layered structures.[30] The interaction of CVB with single metal particles can tailor the relative weight of multipolar plasmon resonances[31] and has been shown to be useful for optical imaging of plasmonic particles[32] especially through second harmonic generation.[33] Here we show that the field distribution at the focus of AP and RP beams enables the efficient excitation of dark modes in highly symmetric clusters of metallic nanoparticles. Incorporating the rigorous description of focused CVB into fully electrodynamic simulations, the near-field and far-field properties of the generated dark modes are analyzed. It is shown that the intensity enhancement due to plasmon coupling can be much larger than the one obtained in bright modes excited with homogeneous illumination. Besides, the distribution of the near field can be qualitatively different, including the formation of areas with very low field intensity. Furthermore, CVB enable the excitation of Fano-like resonances in highly symmetric plasmonic clusters, as result of the coupling of broad and narrow coupled modes of different multipolar order sharing similar charge distribution.

RESULTS AND DISCUSSION

To study the electromagnetic response of a cluster of spherical particles we use the generalized multiparticle Mie theory,[34,35] that is, an electrodynamic semianalytical approach (see Methods section for a detailed discussion). The key idea of this method is the expansion of all the fields in terms of vector spherical harmonics in order to easily impose boundary conditions and solve the electromagnetic problem. Thus, the approach can be used to study the interaction of particles with arbitrary radiation provided that an expansion of the incident field in vector spherical harmonics is available. The generalized multiparticle Mie theory has been widely used for studying the properties of plasmonic systems excited by plane waves. For focused radiation, the inhomogeneous light distribution at focus may change the response of the particles. The field in the focal region of an aplanatic optical system can be rigorously calculated by the diffraction integrals developed by Richards and Wolf.[36] The multipolar expansion of these integrals[37] enables easy expression of the incident field in terms of vector spherical harmonics, which has been used to calculate the electromagnetic response of single particles[38] and particle dimers[39] excited by tightly focused linearly polarized beams. Recently, multipolar expansions for the field distribution of focused cylindrical vector beams have been provided by different authors.[40,41] Incorporating these expansions in the generalized multiparticle Mie theory formalism, we are able to calculate the electromagnetic response of metal nanoparticle clusters excited by CVB. Although the definitions of extinction, scattering, and absorption cross sections typically employed for plane wave excitation cannot be applied to focused beams, one can calculate the power scattered and absorbed by the particles and their sum (henceforth considered as extinguished power) by proper integration of the Poynting vectors.[38] Explicit expressions for the expansion coefficients for the incident field as well as for the scattered, absorbed, and extinguished power are given in the Methods section.

First, we study the response of a dimer made of two silver particles with radius $R = 25$ nm separated a distance $d = 10$ nm. The particles are placed at the focal plane ($z = 0$) and symmetrically located on the x-axis; that is, the particle centers are at $y = 0$ and $x = \pm 30$ nm. The particles are embedded in a medium with refractive index 1.5, and their optical constants are taken from literature.[42] The focusing system consists of an aplanatic lens with a moderate numerical aperture, NA = 0.75, corresponding to a lens semiaperture of 30°. The extinguished power spectrum (Figure 1a) and the near field intensity enhancement (Figure 1b) of the dimer when the lens is illuminated by focused linearly polarized plane waves are characterized by the excitation of bright coupled modes. For a beam polarized in the x-direction, the peak at 2.53 eV corresponds to the in-phase coupling of the dipolar modes of both particles, that is, a bonding mode with azimuthal quantum number $m = 0$ (dimer axis parallel to the excitation polarization) in the plasmon hybridization formalism.[4] If the beam is polarized in the y direction the response is characterized by a peak at 2.93 eV, corresponding also to an in-phase coupling of dipolar moments of the particles but with dipolar moments perpendicular to the dimer axis, that is, an antibonding mode with $m = 1$. Since the numerical aperture of the system is moderate, these results are quantitatively similar to the case of plane wave excitation.[38,39] Next, we assume that the lens is illuminated by an AP beam. In this case the spectra are dominated by a resonance at 2.76 eV. In this situation, the field distribution at the focal plane[43] indicates that the field acting on the particles is primarily perpendicular to the dimer axis and with opposite directions at each particle. Therefore we can associate this resonance to the out-of phase coupling of dipole moments perpendicular to the dimer axis, namely, a bonding mode with $m = 1$. Being a dark mode, its radiative damping is small and the resonance is narrow, with a relative weight of absorption in the extinguished power spectrum larger than for bright modes. It also results in a strong field enhancement, nearly 1 order of magnitude larger than for the bright

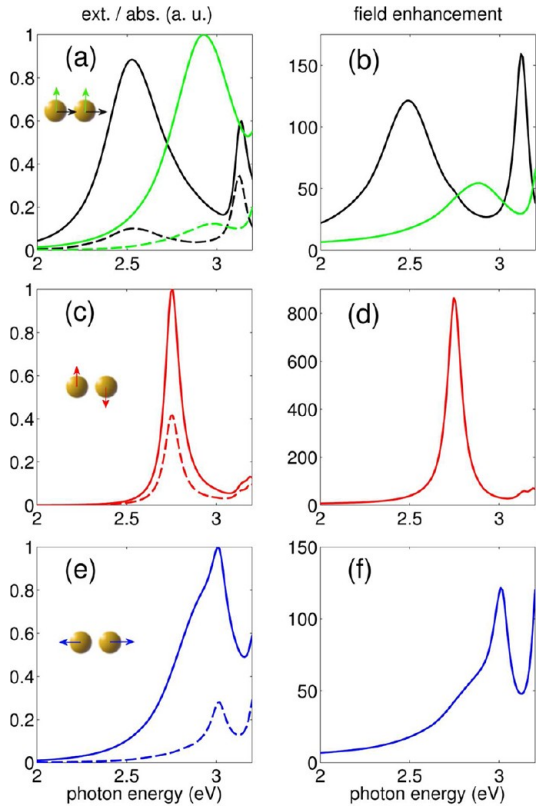

Figure 1. Extinguished (solid lines) and absorbed (dashed lines) power (a, c, e) and near-field intensity enhancement over the particle surfaces normalized to the average intensity acting on each particle (b, d, f) for a particle dimer with radius $R = 25$ and interparticle distance $d = 10$ nm located on the x-axis of the focal plane. The lens is illuminated by plane waves (a, b) polarized in the x (black) or y (green) directions, an AP beam (c, d) and a RP beam (e, f). Arrows indicate the direction of the transversal electric field acting on the particle center.

mode. Finally, if the lens is excited by a RP beam, the spectra show a peak at 3.01 eV. Taking into account that the field acting on each particle is now basically parallel to the dimer axis and with opposite directions in each particle, the resonance can be associated with an antibonding mode with $m = 0$. Since the field generated by each particle opposes the dipolar moment of the other particle, coupling is weak and the field enhancement is moderate compared to the case with AP illumination. In addition to this resonance, a shoulder at slightly lower energies can be distinguished suggesting the excitation of another resonance. Actually, it corresponds to the in-phase antibonding mode with $m = 1$ due to the remarkable longitudinal component (z direction) generated at the focus of RP beams.[44]

To get a deeper insight on the characteristics of dark plasmon modes excited by CVB, the near field intensity maps at the photon energy where the average field enhancement is maximal are shown in Figure 2. For a focused x-polarized plane wave there is a strong field enhancement at center of the dimer, that is, a hot spot is formed due to the large accumulation of charges with opposite signs at the regions of the particle surface facing the dimer gap[45,46] (see Supporting Information for movies of the surface charge distribution oscillations). The y-polarized plane wave does not induce significant enhancement as no large charge gradients are generated. The differences between the two cases can be associated to the near-field coupling, that is the most intense when the polarization of incident light is parallel to the dimer axis.[47] The excitation with an AP beam is shown in Figure 2.c. Although the average enhancement is nearly 1 order of magnitude larger than the one obtained with an x-polarized plane wave (Figure 1), the maximum field enhancements are comparable. Qualitatively, the field distribution is close to the y-polarized plane wave excitation, that is, the field distribution basically resembles to two y-oriented dipoles, with some distortion due to the weak near field coupling. However, for an AP beam the field generated by each particle reinforces the dipolar moment of the other particle, leading to a much larger enhancement than for the y-polarized plane wave case. We have verified that for dimers with smaller interparticle distance, the field enhancement obtained with x-polarized plane waves can be larger than for an AP beam, but always restricted to the gap region. Therefore, dark modes excited by AP beams can be of interest for sensing applications if a large average field enhancement is sought at relatively large interparticle separations in order, for instance, to avoid the possibility of nonlocal effects.[48] Although weak, the near field coupling for the AP excitation is not negligible and the largest enhancement takes place in the region located between particles. Yet, no charge accumulation occurs at the regions of the particles directly facing each other (see movie in Supporting Information) and a "cold spot", that is, an area with low field intensity, is generated at the center of the dimer. Cold spots have been recently studied in gold nanocubes and they have shown potential for imaging and spectroscopy due to their tight confinement.[49] Indeed, one can observe that the cold spot generated by the AP beam is significantly more localized than the hot spot resulting from the illumination with x-polarized plane wave. Figure 2d, shows the near field distribution for the RP beam excitation. In this case, the strong near field coupling between particles results in destructive interference at the particle junction, and this dark mode has limited potential for field enhancement based applications.

As mentioned above, using a focused RP beam leads to the excitation not only of a dark antibonding mode with $m = 0$, but of a bright antibonding mode with $m = 1$ due to the longitudinal component of the field at focus. Since this component becomes larger the tighter the focusing is,[44] increasing the numerical aperture of the system leads to a more enhanced excitation

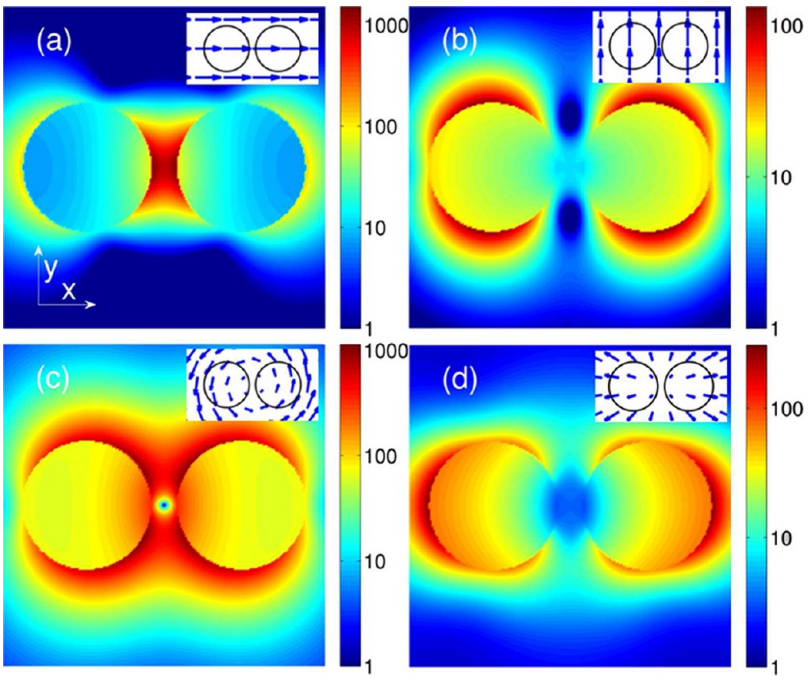

Figure 2. Near field intensity maps (normalized to the average intensity over the particle surface) at the focal plane for a silver dimer with R = 25 nm and d = 10 nm at the photon energy where the average field enhancement (Figure 1) is maximum: (a) x-polarized plane wave, (b) y-polarized plane wave, (c) AP beam, and (d) RP beam. Insets show the distribution of the incident field with polarization contained in the in the focal plane.

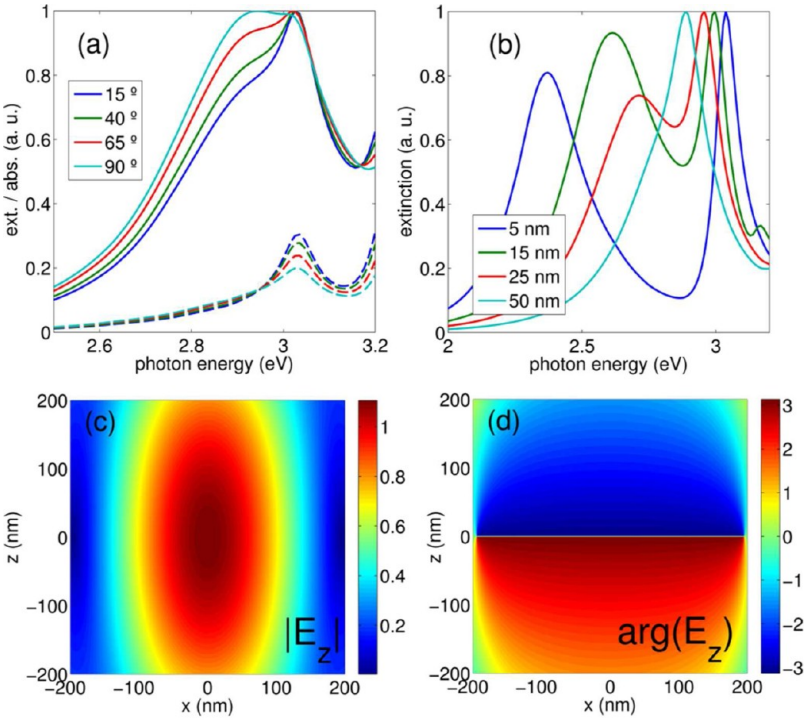

Figure 3. Extinguished (solid lines) and absorbed (dashed lines) power due to the illumination with a focused RP on a dimer with R = 25 nm (a) located on the x-axis and with d = 5 nm and different lens semiapertures, (b) located on the z-axis with varying d and semiaperture of 90°. (c) Amplitude and (d) phase of the longitudinal component of the focused field.

of the antibonding mode with m = 1, as shown in Figure 3a for a dimer with R = 25 nm and d = 5 nm. One should note that in a focused AP beam there is no longitudinal component[43] and the bonding m = 1 mode is the only one excited (Figure 1a). Since the appearance of a longitudinal field component is inherent to focusing a beam with a phase jump in the direction of polarization,[44] the antibonding modes

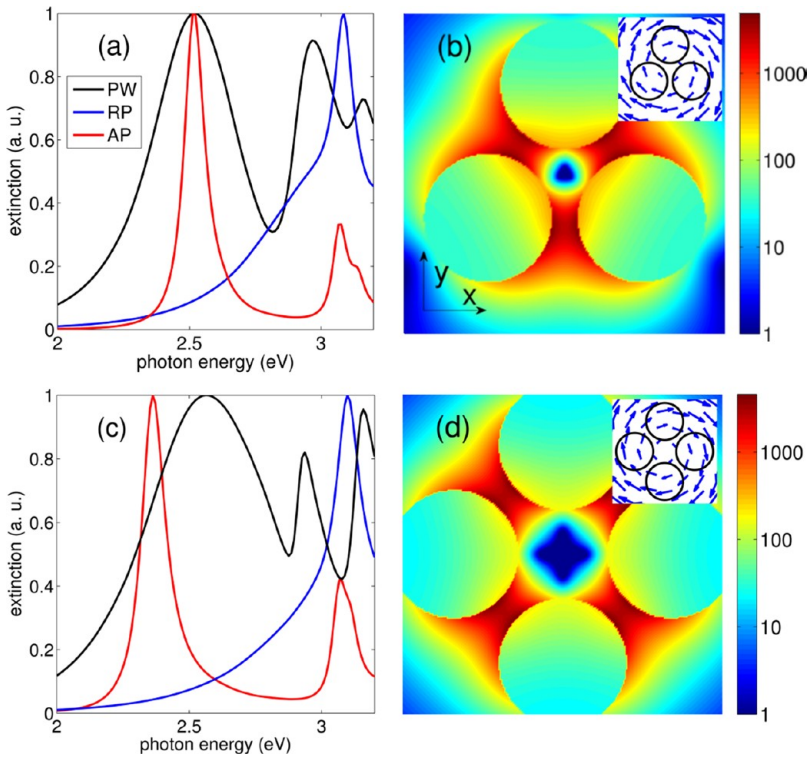

Figure 4. Extinguished power due to the illumination with an *x*-polarized plane wave, AP and RP beam on a (a) silver trimer, (c) silver quadrumer with $R = 25$ nm, $d = 10$ nm. The semiaperture of the lens is 30°. Near field distributions for the trimer (b) and quadrumer (d) excited by an AP beam for the photon energy with largest extinction. Insets show the distribution of the incident field with polarization contained in the in the focal plane.

with $m = 0$ and $m = 1$ cannot be clearly distinguished as they spectrally overlap. However, the longitudinal component of the field enables the efficient excitation of the dark antibonding $m = 0$ mode if the dimer is located at the z axis, at $x = y = 0$ and $z = \pm(R + d/2)$. In this situation the particles are primarily influenced by the longitudinal field component and only the modes with $m = 0$ can be excited. Figure 3b shows the excitation of the bonding (red-shifted peak) and antibonding (blue-shifted peak) for a dimer with $R =$ 25 nm, maximum angular semiaperture, and changing the interparticle distance. In opposition to the case of a dimer placed on the x-axis and illuminated by an x-polarized plane wave (Figure 1a), the dark mode can be excited because the phase of the longitudinal component is not constant through the z-axis (Figure 3d). This implies that the fields acting over the particles are partly in-phase and partly out-of-phase over one period and both modes can be excited. Since the bright $m = 0$ mode is significantly red-shifted with respect to the dark $m = 1$ mode, both resonances can be clearly resolved when the particles are under the influence of the longitudinal field component.

The excitation of dark modes of dimers described above is related to the phase jump existing at the gap separating the particles. Qualitatively similar results could be obtained if other illuminations with phase jumps are used, like Hermite−Gauss beams.[22] CVBs, however, can give place to dark modes in more complex highly symmetric clusters. Figure 4 shows the extinguished power spectra for a trimer and a quadrumer made of silver particles with $R = 25$ nm and $d = 10$ nm excited by x-polarized plane wave, AP and RP beams. The excitation of these plasmonic oligomers by plane waves has been previously discussed,[50] and the broad peak observed at small photon energies corresponds to the admixture of several plasmon modes corresponding to the same irreducible representation in group theory (E' and E_u modes for the trimer and quadrumer).[50] The narrow peaks excited by CVB correspond to a different group symmetry (A_1' and A_{1g} for RP and A_2' and A_{2g} for AP) that cannot be mixed with other modes and are optically inactive for illumination with homogeneous polarization. The excitation of these dark modes enables a large field enhancement at the gaps separating the particles. Compared to the dimer case, now the geometrical arrangement of the particles allows the formation of hot spots, with a maximum intensity enhancement being about 1 order of magnitude larger than for x-polarized plane wave excitation. As in the dimer case, no charge is excited in the area of the particle surface directly facing the center of the oligomer, leading to the formation of cold spots. The dark resonances excited by AP beams can be considered as magnetic modes, as the magnetic dipolar moment[51,52] of the structure is oriented in the

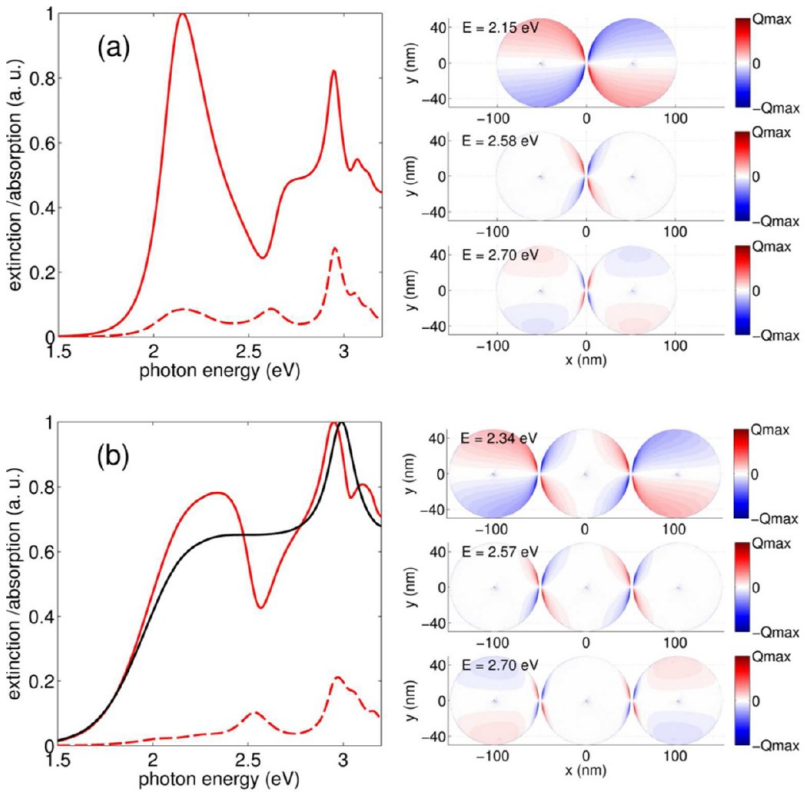

Figure 5. Extinguished (solid line) and absorbed (dashed line) power due to the illumination with a focused AP beam on (a) silver dimer with $R = 50$ nm and $d = 3$ nm, (b) silver dimer with $R = 50$ nm and $d = 106$ nm (black line) and silver trimer with $R = 50$ nm and $d = 3$ nm (red lines). Right panel shows charge distributions at different photon energies for the silver dimer and trimer.

direction of the strong longitudinal magnetic field component.[53]

The small particle sizes of the clusters investigated above allows classification of the modes excited by CVB as dark. For larger particles, retardation becomes important and radiative damping can be significant.[54] Figure 5 shows the extinguished and absorbed power for a dimer with $R = 50$ nm and $d = 3$ nm located at the x-axis and excited by an AP beam focused by a lens with semiaperture 90°. The resonance corresponding with the out-of-phase coupling of the dipolar moments (2.15 eV) is broader than in previous cases (Figure 1) due to the larger particle size, enabling spectral overlapping with modes of higher multipolar order. In this configuration, a pronounced dip appears in the extinguished power spectrum at photon energy of 2.58 eV, that roughly coincides with a maximum in the absorption spectra. This absorption peak corresponds to the coupling of quadrupolar moments of the particles and the dip results from the interference of this resonance with the broad out-of-phase dipole coupling mode, that is, it can be associated to a Fano resonance. The possibility to obtain a Fano dip in the dimer spectra is enabled by the strong spatial overlapping of the charge distribution of the involved resonances. The out-of-phase coupled-dipole resonance results in a charge distribution preferentially confined around the particle gap due to near field interaction (top right panel, Figure 5a) and shares certain similarity with the coupled-quadrupole resonance (low panel in Figure 5a). Thus, phase toggling takes place as the photon energy is varied through the coupled-quadrupole resonance,[55] with an efficient destructive interference and strong charge localization around the dimer gap when the Fano minimum occurs (middle panel). A dimer excited by a linearly polarized plane wave does not show such pronounced dips[56] as the charge distribution of the in-phase coupling modes of different orders do not show significant spatial overlapping. The Fano minimum appearing in the Ag dimer in Figure 5a can be enhanced if the resonance playing the role of continuum is further broadened. By placing the two particles at larger distance (black line in Figure 5b), the coupling is reduced and the extinction spectrum shows a broad peak, resembling the dipolar excitation of a single particle. If a third particle is located at the center of such a dimer, the dipolar mode is only slightly perturbed since the field acting on the central particle at the origin vanishes and the resonance is still broad. However, the central particle enables strong coupling of the quadrupole moments of the particles, leading to a dip in the extinguished power spectra (2.57 eV). The excitation of Fano resonances in plasmonic systems usually requires a certain degree of asymmetry or complexity in the structure; however, the present simulations reveal that CVB could

be used to generate such resonances in relatively simple and symmetric systems.

CONCLUSION

We have shown that focused AP and RP beams can be used to efficiently excite dark plasmon modes in nanoparticle clusters, having reduced radiative damping and larger field enhancement with respect to bright modes. The near field distribution resulting from CVB excitation is highly inhomogeneous and includes regions with large field enhancement and electromagnetic cold spots. Finally, the spatial overlapping of the charge distribution of coupled multipolar resonances of different order gives place to Fano dips in the extinction spectrum of symmetric clusters such as dimers. Being that these properties are unattainable with linearly polarized beams, our results show that CVB can be used to further exploit the application potential of plasmonic clusters.

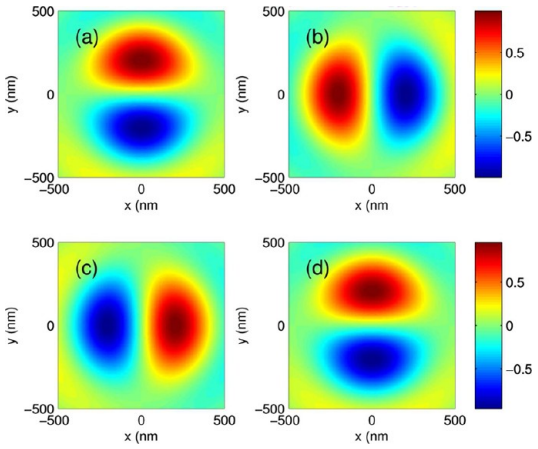

Figure 6. Distribution of field at the focal plane of a lens with angular semiaperture 30° in a medium with refractive index $n = 1.5$ illuminated by an azimuthally polarized (a, b) and radially polarized (c, d) beams. The *x*-polarization components are shown in panels a and c, and the y-polarization components are shown in panels b and d.

METHODS

The generalized multiparticle Mie theory[34,35] consists on expanding the incident ($\mathbf{E}_0$), scattered ($\mathbf{E}_S$) and internal ($\mathbf{E}_I$) fields in series of vector spherical harmonics $\mathbf{m}_{pq1(3)}$ and $\mathbf{n}_{pq1(3)}$ defined with respect to the center of the particle *i*.

$$\mathbf{E}_0^i(\mathbf{r}_i) = \sum_{q=1}^{\infty}\sum_{p=-q}^{q} a_{pq}^i \mathbf{m}_{pq1}^i(\mathbf{r}_i) + b_{pq}^i \mathbf{n}_{pq1}^i(\mathbf{r}_i) \quad (1)$$

$$\mathbf{E}_S^i(\mathbf{r}_i) = \sum_{q=1}^{\infty}\sum_{p=-q}^{q} c_{pq}^i \mathbf{m}_{pq3}^i(\mathbf{r}_i) + d_{pq}^i \mathbf{n}_{pq3}^i(\mathbf{r}_i) \quad (2)$$

$$\mathbf{E}_I^i(\mathbf{r}_i) = \sum_{q=1}^{\infty}\sum_{p=-q}^{q} e_{pq}^i \mathbf{m}_{pq1}^i(\mathbf{r}_i) + f_{pq}^i \mathbf{n}_{pq1}^i(\mathbf{r}_i) \quad (3)$$

We employ the definition of vectors spherical harmonics of Gérardy and Ausloos.[34] The index 1 or 3 in the vector spherical harmonics refers to the Bessel function taken to guarantee finiteness at origin (for the internal and incident field) or at infinite (scattered fields). Taking into account that the field acting over each particle is the sum of the incident field and the field scattered by all the other particles and imposing boundary conditions at the all the particle surfaces, a linear system connecting the scattered with incident field coefficients results:

$$d_{lm}^j - \Delta_l^j \sum_{q,p}\sum_{i\neq j}^{N} [c_{qp}^i \mathbf{C}_{qplm}^{ij} + d_{qp}^i \mathbf{T}_{qplm}^{ij}] = \Delta_l^j b_{lm}^j \quad (4)$$

where N is the number of particles and the matrices $\mathbf{C}_{qplm}^{ij}$ and $\mathbf{T}_{qplm}^{ij}$ are result of vector addition theorems and connect the vector spherical harmonics defined at different origins, that is, centered at different particles. By truncating the system to a maximum degree q_{max}, the scattering coefficients can be determined. The value of q_{max} depends on the particle size and the strength of the electromagnetic coupling among particles. In our simulations q_{max} has been varied until convergence of the computed far-field or near-field quantities was achieved.

A multipolar expansion for a focused cylindrical vector beam was developed by Borghi *et al.*[40] Owing to the symmetry of such beams, only vector spherical harmonics with $q = 0$ are needed. In particular, a radially polarized beam is determined by $b_{q0}^0 = A(q)$ and $a_{q0}^0 = 0$, while an azimuthally polarized beam require $a_{q0}^0 = A(q)$ and $b_{q0}^0 = 0$, with

$$A(q) = i^q \sqrt{2q+1} \int_0^{\alpha} \exp\left(\frac{-f\sin\theta}{w}\right)^2 \frac{f}{w} \sin^2\theta \sqrt{\cos\theta} P_q^1(\cos\theta)\, d\theta \quad (5)$$

where α is the angular semiaperture of the lens, f is its focal number, and w is the beam waist. In our calculations we have considered $f = w$. The multipolar expansion for focused cylindrical vector beams has its origin at the focus, and vector addition theorems are necessary to calculate the expansion coefficients with origin at different particle centers. Figure 6 shows the distribution of the field at the focal plane for AP and RP beams calculated using the multipolar expansion.

For plane wave illumination, extinction, absorption, and scattering are usually quantified through cross sections, defined as the ratio of extinguished, absorbed, and scattered power with respect to the incident irradiance. For a nonhomogeneous illumination this definition losses its meaning, but it is possible to calculate the total power scattered (P_{sca}) and the sum of absorbed and scattered power ($P_{sca+abs}$) in the same way as for plane waves.[38]

$$P_{sca} = \frac{1}{2Zk^2}\sum_{i,q,p}\left\{|c_{qp}^i|^2 + |d_{qp}^i|^2 + Re\left[\left(\frac{c_{qp}^i}{\Gamma_q^i} - a_{qp}^i\right)c_{qp}^{i*} + \left(\frac{d_{qp}^i}{\Delta_q^i} - b_{qp}^i\right)d_{qp}^{i*}\right]\right\} \quad (6)$$

$$P_{sca+abs} = -\frac{1}{2Zk^2}\sum_{i,q,p} Re[a_{qp}^i c_{qp}^{i*} + b_{qp}^i d_{qp}^{i*}] \quad (7)$$

where Z is the medium impedance. $P_{sca+abs}$ can be identified with the extinguished power, and the absorbed power, P_{abs} can be calculated as $P_{sca+abs} - P_{sca}$. Expressions 6 and 7 have been used through the article in order to quantify the far-field response of metal nanoparticles excited by cylindrical vector beams.

Conflict of Interest: The authors declare no competing financial interest.

Acknowledgment. J.S.P. acknowledges the financial support of the Government of Catalonia through a "Beatriu de Pinós" grant.

Supporting Information Available: Movies of the surface charge distribution of the plasmon dark and bright modes in dimers. This material is available free of charge *via* the Internet at http://pubs.acs.org.

REFERENCES AND NOTES

1. Maier, S. *Plasmonics: Fundamentals and Applications*; Springer: New York, 2007.
2. Kelly, K. L.; Coronado, E.; Zhao, L. L.; Schatz, G. C. The Optical Properties of Metal Nanoparticles: The Influence of Size, Shape, and Dielectric Environment. *J. Phys. Chem. B* **2002**, *107*, 668–677.
3. Chu, M.-W.; Myroshnychenko, V.; Chen, C. H.; Deng, J.-P.; Mou, C.-Y.; García de Abajo, F. J. Probing Bright and Dark Surface-Plasmon Modes in Individual and Coupled Noble Metal Nanoparticles Using an Electron Beam. *Nano Lett.* **2008**, *9*, 399–404.
4. Nordlander, P.; Oubre, C.; Prodan, E.; Li, K.; Stockman, M. I. Plasmon Hybridization in Nanoparticle Dimers. *Nano Lett.* **2004**, *4*, 899–903.
5. Liu, M.; Lee, T.-W.; Gray, S. K.; Guyot-Sionnest, P.; Pelton, M. Excitation of Dark Plasmons in Metal Nanoparticles by a Localized Emitter. *Phys. Rev. Lett.* **2009**, *102*, 107401.
6. Halas, N. J.; Lal, S.; Chang, W.-S.; Link, S.; Nordlander, P. Plasmons in Strongly Coupled Metallic Nanostructures. *Chem. Rev.* **2011**, *111*, 3913–3961.
7. Solis, D.; Willingham, B.; Nauert, S. L.; Slaughter, L. S.; Olson, J.; Swanglap, P.; Paul, A.; Chang, W.-S.; Link, S. Electromagnetic Energy Transport in Nanoparticle Chains *via* Dark Plasmon Modes. *Nano Lett.* **2012**, *12*, 1349–1353.
8. Luk'yanchuk, B.; Zheludev, N. I.; Maier, S. A.; Halas, N. J.; Nordlander, P.; Giessen, H.; Chong, C. T. The Fano Resonance in Plasmonic Nanostructures and Metamaterials. *Nat. Mater.* **2010**, *9*, 707–715.
9. Miroshnichenko, A. E.; Flach, S.; Kivshar, Y. S. Fano Resonances in Nanoscale Structures. *Rev. Mod. Phys.* **2010**, *82*, 2257–2298.
10. Hao, F.; Sonnefraud, Y.; Dorpe, P. V.; Maier, S. A.; Halas, N. J.; Nordlander, P. Symmetry Breaking in Plasmonic Nanocavities: Subradiant LSPR Sensing and a Tunable Fano Resonance. *Nano Lett.* **2008**, *8*, 3983–3988.
11. Verellen, N.; Sonnefraud, Y.; Sobhani, H.; Hao, F.; Moshchalkov, V. V.; Dorpe, P. V.; Nordlander, P.; Maier, S. A. Fano Resonances in Individual Coherent Plasmonic Nanocavities. *Nano Lett.* **2009**, *9*, 1663–1667.
12. Hentschel, M.; Saliba, M.; Vogelgesang, R.; Giessen, H.; Alivisatos, A. P.; Liu, N. Transition from Isolated to Collective Modes in Plasmonic Oligomers. *Nano Lett.* **2010**, *10*, 2721–2726.
13. Mukherjee, S.; Sobhani, H.; Lassiter, J. B.; Bardhan, R.; Nordlander, P.; Halas, N. J. Fanoshells: Nanoparticles with Built-in Fano Resonances. *Nano Lett.* **2010**, *10*, 2694–2701.
14. Rahmani, M.; Lukiyanchuk, B.; Ng, B.; Tavakkoli K. G, A.; Liew, Y. F.; Hong, M. H. Generation of Pronounced Fano Resonances and Tuning of Subwavelength Spatial Light Distribution in Plasmonic Pentamers. *Opt. Express* **2011**, *19*, 4949–4956.
15. Sheikholeslami, S.; Jun, Y.-w.; Jain, P. K.; Alivisatos, A. P. Coupling of Optical Resonances in a Compositionally Asymmetric Plasmonic Nanoparticle Dimer. *Nano Lett.* **2010**, *10*, 2655–2660.
16. Sonnefraud, Y.; Verellen, N.; Sobhani, H.; Vandenbosch, G. A. E.; Moshchalkov, V. V.; Van Dorpe, P.; Nordlander, P.; Maier, S. A. Experimental Realization of Subradiant, Superradiant, and Fano Resonances in Ring/Disk Plasmonic Nanocavities. *ACS Nano* **2010**, *4*, 1664–1670.
17. Huang, J.-S.; Kern, J.; Geisler, P.; Weinmann, P.; Kamp, M.; Forchel, A.; Biagioni, P.; Hecht, B. Mode Imaging and Selection in Strongly Coupled Nanoantennas. *Nano Lett.* **2010**, *10*, 2105–2110.
18. Yang, S.-C.; Kobori, H.; He, C.-L.; Lin, M.-H.; Chen, H.-Y.; Li, C.; Kanehara, M.; Teranishi, T.; Gwo, S. Plasmon Hybridization in Individual Gold Nanocrystal Dimers: Direct Observation of Bright and Dark Modes. *Nano Lett.* **2010**, *10*, 632–637.
19. Zhou, W.; Odom, T. W. Tunable Subradiant Lattice Plasmons by Out-of-Plane Dipolar Interactions. *Nat. Nanotechnol.* **2011**, *6*), 423–427.
20. Hao, F.; Larsson, E. M.; Ali, T. A.; Sutherland, D. S.; Nordlander, P. Shedding Light on Dark Plasmons in Gold Nanorings. *Chem. Phys. Lett.* **2008**, *458*, 262–266.
21. Rolly, B.; Stout, B.; Bonod, N. Metallic dimers: When Bonding Transverse Modes Shine Light. *Phys. Rev. B* **2011**, *84*, 125420.
22. Volpe, G.; Cherukulappurath, S.; Juanola Parramon, R.; Molina-Terriza, G.; Quidant, R. Controlling the Optical Near Field of Nanoantennas with Spatial Phase-Shaped Beams. *Nano Lett.* **2009**, *9*, 3608–3611.
23. Su, X.-R.; Zhang, Z.-S.; Zhang, L.-H.; Li, Q.-Q.; Chen, C.-C.; Yang, Z.-J.; Wang, Q.-Q. Plasmonic Interferences and Optical Modulations in Dark–Bright–Dark Plasmon Resonators. *Appl. Phys. Lett.* **2010**, *96*, 043113–3.
24. Aeschlimann, M.; Bauer, M.; Bayer, D.; Brixner, T.; Garcia de Abajo, F. J.; Pfeiffer, W.; Rohmer, M.; Spindler, C.; Steeb, F. Adaptive Subwavelength Control of Nano-optical Fields. *Nature* **2007**, *446*, 301–304.
25. Volpe, G.; Molina-Terriza, G.; Quidant, R. Deterministic Subwavelength Control of Light Confinement in Nanostructures. *Phys. Rev. Lett.* **2010**, *105*, 216802.
26. Kao, T. S.; Rogers, E. T. F.; Ou, J. Y.; Zheludev, N. I. Digitally Addressable Focusing of Light into a Subwavelength Hot Spot. *Nano Lett.* **2012**, *12*, 2728–2731.
27. Kao, T. S.; Jenkins, S. D.; Ruostekoski, J.; Zheludev, N. I. Coherent Control of Nanoscale Light Localization in Metamaterial: Creating and Positioning Isolated Subwavelength Energy Hot Spots. *Phys. Rev. Lett.* **2011**, *106*, 085501.
28. Boriskina, S. V.; Reinhard, B. M. Molding the Flow of Light on the Nanoscale: From Vortex Nanogears to Phase-Operated Plasmonic Machinery. *Nanoscale* **2012**, *4*, 76–90.
29. Ahn, W.; Boriskina, S. V.; Hong, Y.; Reinhard, B. M. Electromagnetic Field Enhancement and Spectrum Shaping through Plasmonically Integrated Optical Vortices. *Nano Lett.* **2011**, *12*, 219–227.
30. Zhan, Q. Cylindrical Vector Beams: From Mathematical Concepts to Applications. *Adv. Opt. Photon.* **2009**, *1*, 1–57.
31. Mojarad, N. M.; Agio, M. Tailoring the Excitation of Localized Surface Plasmon–Polariton Resonances by Focusing Radially-Polarized Beams. *Opt. Express* **2009**, *17*, 117–122.
32. Failla, A. V.; Qian, H.; Qian, H.; Hartschuh, A.; Meixner, A. J. Orientational Imaging of Subwavelength Au Particles with Higher Order Laser Modes. *Nano Lett.* **2006**, *6*, 1374–1378.
33. Bautista, G.; Huttunen, M. J.; Mäkitalo, J.; Kontio, J. M.; Simonen, J.; Kauranen, M. Second-Harmonic Generation Imaging of Metal Nano-objects with Cylindrical Vector Beams. *Nano Lett.* **2012**, *12*, 3207–3212.
34. Gérardy, J. M.; Ausloos, M. Absorption Spectrum of Clusters of Spheres from the General Solution of Maxwell's Equations. II. Optical Properties of Aggregated Metal Spheres. *Phys. Rev. B* **1982**, *25*, 4204–4229.
35. Xu, Y.-l. Electromagnetic Scattering by an Aggregate of Spheres. *Appl. Opt.* **1995**, *34*, 4573–4588.
36. Richards, B.; Wolf, E. Electromagnetic Diffraction in Optical Systems. II. Structure of the Image Field in an Aplanatic System. *Proc. R. Soc. London, Ser. A.* **1959**, *253*, 358–379.
37. Sheppard, C. J. R.; Török, P. Efficient Calculation of Electromagnetic Diffraction in Optical Systems Using a Multipole Expansion. *J. Mod. Opt.* **1997**, *44*, 803–818.
38. Mojarad, N. M.; Sandoghdar, V.; Agio, M. Plasmon Spectra of Nanospheres under a Tightly Focused Beam. *J. Opt. Soc. Am. B* **2008**, *25*, 651–658.
39. Sancho-Parramon, J. Near-Field Coupling of Metal Nanoparticles under Tightly Focused Illumination. *Opt. Lett.* **2011**, *36*, 3527–3529.
40. Borghi, R.; Santarsiero, M.; Alonso, M. A. Highly Focused Spirally Polarized Beams. *J. Opt. Soc. Am. A* **2005**, *22*, 1420–1431.
41. Hoang, T. X.; Chen, X.; Sheppard, C. J. R. Multipole Theory for Tight Focusing of Polarized Light, Including Radially Polarized and Other Special Cases. *J. Opt. Soc. Am. A* **2012**, *29*, 32–43.

42. Johnson, P. B.; Christy, R. W. Optical Constants of the Noble Metals. *Phys. Rev. B* **1972**, *6*, 4370–4379.
43. Youngworth, K.; Brown, T. Focusing of High Numerical Aperture Cylindrical-Vector Beams. *Opt. Express* **2000**, *7*, 77–87.
44. Novotny, L.; Hecht, B. *Principles of Nano-optics*; Cambridge University Press: Cambridge, UK, 2006.
45. Romero, I.; Aizpurua, J.; Bryant, G. W.; García De Abajo, F. J. Plasmons in Nearly Touching Metallic Nanoparticles: Singular Response in the Limit of Touching Dimers. *Opt. Express* **2006**, *14*, 9988–9999.
46. Hao, E.; Schatz, G. C. Electromagnetic Fields around Silver Nanoparticles and Dimers. *J. Chem. Phys.* **2004**, *120*, 357–366.
47. Pinchuk, A. O.; Schatz, G. C. Nanoparticle Optical Properties: Far- and Near-Field Electrodynamic Coupling in a Chain of Silver Spherical Nanoparticles. *Mater. Sci. Eng., B* **2008**, *149*, 251–258.
48. Alvarez-Puebla, R. n.; Liz-Marzán, L. M.; García de Abajo, F. J. Light Concentration at the Nanometer Scale. *J. Phys. Chem. Lett.* **2010**, *1*, 2428–2434.
49. Haggui, M.; Dridi, M.; Plain, J.; Marguet, S.; Perez, H.; Schatz, G. C.; Wiederrecht, G. P.; Gray, S. K.; Bachelot, R. Spatial Confinement of Electromagnetic Hot and Cold Spots in Gold Nanocubes. *ACS Nano* **2012**, *6*, 1299–1307.
50. Brandl, D. W.; Mirin, N. A.; Nordlander, P. Plasmon Modes of Nanosphere Trimers and Quadrumers. *J. Phys. Chem. B* **2006**, *110*, 12302–12310.
51. Sheikholeslami, S. N.; García-Etxarri, A.; Dionne, J. A. Controlling the Interplay of Electric and Magnetic Modes *via* Fano-like Plasmon Resonances. *Nano Lett.* **2011**, *11*, 3927–3934.
52. Alù, A.; Salandrino, A.; Engheta, N. Negative Effective Permeability and Left-Handed Materials at Optical Frequencies. *Opt. Express* **2006**, *14*, 1557–1567.
53. Novotny, L.; Beversluis, M. R.; Youngworth, K. S.; Brown, T. G. Longitudinal Field Modes Probed by Single Molecules. *Phys. Rev. Lett.* **2001**, *86*, 5251–5254.
54. Dahmen, C.; Schmidt, B.; von Plessen, G. Radiation Damping in Metal Nanoparticle Pairs. *Nano Lett.* **2007**, *7*, 318–322.
55. López-Tejeira, F.; Paniagua-Domínguez, R.; Rodríguez-Oliveros, R.; Sánchez-Gil, J. A. Fano-like Interference of Plasmon Resonances at a Single Rod-Shaped Nanoantenna. *New J. Phys.* **2012**, *14*, 023035.
56. Bao, K.; Mirin, N.; Nordlander, P. Fano Resonances in Planar Silver Nanosphere Clusters. *Appl. Phys. A: Mater. Sci. Process.* **2010**, *100*, 333–339.